# Effects of nonframework metal cations and phonon scattering mechanisms on the thermal transport properties of polycrystalline zeolite LTA films

Abraham Greenstein,[1] Yeny Hudiono,[2] Samuel Graham,[1] and Sankar Nair[2,a)]
[1]*Woodruff School of Mechanical Engineering, Georgia Institute of Technology, Atlanta, Georgia 30332-0405, USA*
[2]*School of Chemical & Biomolecular Engineering, Georgia Institute of Technology, Atlanta, Georgia 30332-0100, USA*

(Received 8 June 2009; accepted 24 January 2010; published online 31 March 2010)

We present a systematic study to investigate the effects of nonframework cations and the role of phonon scattering mechanisms on the thermal transport properties of zeolite LTA, via experiment and semiempirical lattice dynamics calculations. Our study is motivated by the increasing interest in accurate measurements and mechanistic understanding of the thermal transport properties of zeolite materials. The presence of a nanostructured pore network, extra-framework cations, and tunable framework structure and composition confer interesting thermophysical properties to these materials, making them a good model system to investigate thermal transport in complex materials. Continuous films of zeolite LTA with different nonframework cations ($Na^+$, $K^+$, and $Ca^{+2}$) were synthesized and characterized. The thermal conductivity was measured using the three-omega method over a wide range of temperature (150–450 K). These are the first thermal conductivity measurements performed on bulk LTA, so they are more accurate than previous measurements, which involved the use of compacted zeolite powders. Our data showed significant dependence of the thermal conductivity on the extra-framework cations as well the temperature. The thermal conductivities of the zeolite LTA samples were modeled with the relaxation time approximation to the Boltzmann transport equation. The full phonon spectra for each type of LTA zeolite were calculated and used in conjunction with semiempirical relaxation time expressions to calculate the thermal conductivity. The results both validated, and suggested the limitations of, this modeling approach. Optical phonons dominated the thermal conductivity and boundarylike scattering was found to be the strongest phonon scattering mechanism, as also observed in MFI zeolite.
 [doi:10.1063/1.3327419]

## I. INTRODUCTION

Zeolites are nanoporous mixed-oxide crystals with complex structures formed by corner-sharing oxide tetrahedra ($TO_4$; with T=Si, Al, etc.).[1] Approximately 175 zeolite structures can currently be synthesized. A large number of other framework structures can also be obtained by inclusion of elements that favor octahedral and pentahedral coordination. The capability of altering the composition of a given zeolite framework (e.g., by lattice atom substitution or by introducing metal cations and organic molecules into the pores while maintaining the same crystal structure), or conversely the ability to synthesize different crystal structures with the same composition, makes them extraordinarily versatile materials with interesting structure-function relationships[2] and many important applications in the energy and chemical processing sectors.[3] Newly emerging device applications for zeolite materials and thin films include materials for adsorption cooling devices,[4] low-*k* dielectric films for computer chips,[4–6] and patterned nanostructures for optoelectronic applications.[7,8]

Our interest in the thermal transport properties of zeolite materials originates primarily from their suitability as a model system containing complex, yet well-defined and characterizable, nanostructural features (such as an ordered nanopore network, lattice substitution sites, metal cations, or organic species adsorbed in the pores) that interact with heat-carrying phonons. This creates a number of opportunities for developing and testing models of thermal conduction in complex crystals. In a recent work,[9] we have shown that the thermal conductivity of zeolite MFI thin films can be tuned by substituting silicon with aluminum in the zeolite framework. This is due to a reduction in phonon velocity as well as point defect scattering, thus thermal conductivity decreases as the amount of aluminum in the zeolite framework increases. We have also demonstrated that the thermal conductivity of MFI thin films is affected by the presence of the organic template inside the zeolite pores.[10] In this paper we investigate the effects of extra-framework substitutions of metal cations in the zeolite pores, using the aluminosilicate zeolite LTA as the model system. Thermal transport in this system is studied by measuring and modeling the thermal conductivity of polycrystalline films of three cation containing LTA zeolites: Na-LTA, K-LTA, and Ca-LTA.

The thermal conductivity of zeolite LTA powders has previously been investigated by experiment and simulation. Previous experimental studies measured the effective thermal conductivity of compacted powders of Na-LTA.[9,10] Approximate measurement models and data analysis were used to estimate the bulk thermal conductivity of LTA. The resulting

a)Author to whom correspondence should be addressed. Electronic mail: sankar.nair@chbe.gatech.edu.

 

estimates for the thermal conductivity of zeolite Na-LTA from the two studies differ by more than an order of magnitude. More direct measurements of the thermal conductivity of LTA are needed to resolve such discrepancies, and to provide insight into the effects of nonframework cations on thermal properties. There have also been two molecular dynamics simulation studies of the thermal conductivity of bulk zeolite LTA, aimed at a better understanding of thermal transport in complex porous materials.[11,12] McGaughey and Kaviany[11] highlighted the temperature dependence of the thermal conductivity and phonon mean free path in a pure-silica form of LTA. It is currently not possible to synthesize thin films of pure-silica LTA, and therefore their findings cannot yet be directly compared to experiment. Murashov[12] simulated thermal transport in aluminosilicate LTA with different metal cations in the pores. However, the short MD simulation timescale implies that a good statistical sample of the thermal behavior may be difficult to obtain. This was mentioned[13] as a possible reason for the discrepancies between the different simulation studies. Additionally, the thermal properties of zeolite LTA exhibit quantum effects and therefore classical molecular dynamics (MD) simulation results, which have been used very successfully for simple crystals,[13–15] should be treated with some caution.

In this study we address both the need for unambiguous experimental measurements of the thermal conductivity of LTA, and more detailed physical insight into the thermal conduction processes in such nanoporous materials. Our approach is to fabricate polycrystalline Na-LTA films, from which Ca-LTA and K-LTA films can be derived by ion exchange techniques. The films are prepared by secondary (seeded) growth from a spin-coated seed layer of LTA nanoparticles, and are characterized by x-ray diffraction (XRD), scanning electron microscopy (SEM), and energy dispersive spectroscopy (EDS) to determine the crystal structure, out of plane crystal orientation of the film, and nonframework cation content. We then conduct detailed measurements of thermal conductivity as a function of temperature, using the three-omega method. We model the thermal conductivity in the framework of the relaxation time approximation of the Boltzmann transport equation, with detailed input on phonon dispersion and specific heat obtained from atomistic lattice dynamics calculations.

## II. EXPERIMENTAL AND COMPUTATIONAL METHODS

Zeolite LTA (Fig. 1) has a cubic crystal structure, and crystallizes in *Fm3c* space group.[15] The framework of Zeolite A is built by connecting two sodalite cages via oxygen atoms on the four-membered ring faces. The Si:Al ratio is approximately unity. Hence the T-atom positions are alternately occupied by Si and Al, in accordance with Loewenstein's rule.[16] A unit cell of LTA (Fig. 1) contains a large cage with a diameter of 11.4 Å and smaller cages with a diameter of 6.6 Å. The large cages are connected to each other via eight-membered rings. The unit cell also contains six-membered rings and four-membered rings. Three kinds of sites are available for extra-framework cations:[16] the $\alpha$-site located near the center of the eight-membered ring, the $\beta$-site located near the center of six-membered ring, and the $\gamma$-site located near the center of the four-membered ring. In most cases, the $\gamma$-site has the weakest affinity for cations, and $\beta$-site has the highest affinity for cations.[16,17] This paper focuses on three types of cations: $Na^+$, $K^+$, and $Ca^{2+}$. The LTA unit cell has 96 Al atoms, 96 Si atoms, and 384 O atoms, so the net negative charge of the framework is $-96$. The balancing positive charge from the metal cations is therefore +96. $Na^+$ and $K^+$ are monovalent while $Ca^{2+}$ is divalent, hence Na-LTA and K-LTA have 96 cations and Ca-LTA has 48. For each type of LTA, the total number of available cation sites is much larger than the actual number of cations required to balance the framework charge. Hence, the cation distribution among the three types of sites is typically disordered.

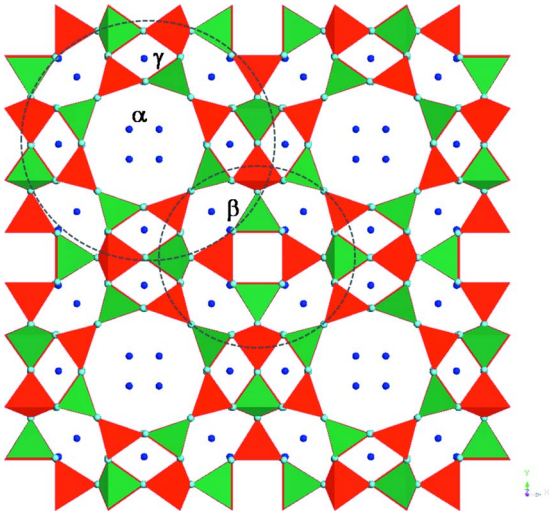


FIG. 1. (Color online) Crystal structure of zeolite Na-LTA. Red: $SiO_4$ tetrahedra, green: $AlO_4$ tetrahedra. Blue spheres located in the pores represent (partially occupied) $Na^+$ cation sites. The large cages and small cages are indicated by dashed circles. The three types of cation sites are labeled.

### A. Zeolite film synthesis and characterization

The synthesis of a continuous LTA zeolite film was involved because the high Al content inhibits the film growth process. The synthesis conditions were manipulated extensively in order to finally obtain a continuous, high-quality Na-LTA film. The Na-LTA seed nanoparticles are prepared from a clear solution with a composition of 4.1 $(TMA)_2O$:0.35 $Na_2O$:1 $Al_2O_3$:3.4 $SiO_2$:239 $H_2O$, as described in detail by Boudreau.[18] LTA zeolite films were prepared using the secondary hydrothermal method. The clear synthesis solution was composed of 4.1 $(TMA)_2O$:0.36 $Na_2O$:1 $Al_2O_3$:4.4 $SiO_2$:706.2 $H_2O$. A 50 g/l suspension of zeolite seed nanoparticles in ethanol was spin-coated on a commercially available alumina substrate (CoorsTek). The substrate was dried at room temperature for 4 h. The synthesis mixture was hydrolyzed at room temperature to achieve a clear solution. The coated substrate was placed in the synthesis solution with the coated side facing downward. The hydrothermal synthesis was performed at 110 °C for three days. The films were washed with warm water, dried at 60 °C for 6 h, and then were then calcined at

500 °C for 8 h with a heating rate of 1 °C/hour. The growth process was repeated twice in order to obtain a thicker LTA zeolite film. The films were polished first with SiC paper (Buehler Inc., 1000 and 4000 grit) at 100 rpm for 20 s and then with alumina polishing suspensions to obtain 0.5, 0.3 and 0.05 $\mu$m smoothness. Ion exchange of the as-synthesized sodium-containing films with potassium or calcium ions was performed by suspending the films vertically in 0.1 M salt solutions containing KCl or $CaCl_2$ at 70 °C for 6 h. This process was repeated three times, and each time a fresh solution was used, the films were first washed with warm water to remove any excess chloride or salt on the surface. The films were characterized by XRD to verify the formation of LTA films. The film morphology, thicknesses, and compositions were characterized by SEM and EDS.

### B. Thermal conductivity measurements

The thermal conductivity of the zeolite LTA films was measured using a three-omega method, as previously discussed.[9] Before measuring the thermal conductivity, the zeolite film sample was first heated under vacuum to 450 K and held overnight. This step was necessary to ensure the complete dehydration of LTA, because it readily adsorbs water at ambient conditions. This procedure also ensured that the thermal conductivity measurement was conducted on the cubic crystal structure of LTA used in the lattice dynamics calculations. It was reported[15] that although the crystal structure of LTA zeolite initially changes upon evacuation and heating, the fully dehydrated structure returns to a cubic crystal and does not change upon further heating or cooling until it is rehydrated.

### C. Structural model and phonon dispersion calculations

The first step in the calculation was to create a representative supercell of the structure. The unit cells used for the calculation are based on detailed literature data[20–22] regarding the cation site locations and occupancies. Most cation sites have only partial occupancies. LTA unit cells modeled by mean field theory (i.e., assuming all the cation sites to be filled with partial occupancies) were found to be unstable. Therefore, the cations were instead placed randomly into different cation sites such that each different type of cation site had the correct overall site occupancy. Furthermore, care was taken to ensure that two neighboring cations were not placed in locations that cannot simultaneously be occupied (due to electrostatic repulsion). To get a statistical sample of the cation positions, a supercell was used to model the crystal structure. The supercells used here were made from four LTA primitive lattice cells, which correspond to what is typically referred to as a single LTA unit cell. To check that a good statistical sample of cation locations in the crystal was obtained with this supercell, three representative unit cells for each type of LTA were created, with different random cation configurations. For each type of LTA studied the three different densities of states for the three different cation configurations were calculated and found to be nearly identical; this implies that the representative unit cells used are reasonable approximation of the actual crystals.

An appropriate interatomic potential must be chosen before performing the lattice dynamical calculations. For LTA the potential model developed by Catlow[19,23] was used because of its many previous computational successes. It includes Buckingham terms for the dipole-dipole interactions of the O–O, Si–O, Al–O, and cation-O bonds, a three body term for angle bending of the $SiO_4$ and $AlO_4$ tetrahedrons, a Coulombic term resulting from the polarity of Si–O and Al–O bonds, and a core-shell model for oxygen atom polarizability. The first step in the calculation was to use the interatomic potential to calculate and minimize the energy of the unit cell. This was done with a combination of the rational function optimizer (RFO) and Newton—Raphson techniques, which were implemented with the general utility lattice program (GULP).[24] During the energy minimizations, the fractional coordinates of all framework and nonframework atoms in the representative unit cell were allowed to relax and the unit cell parameters were left constant at the values obtained from the crystal diffraction data in the literature. The potential energy surface had many saddle points. Therefore, care was taken when analyzing the results. If all the phonon frequencies are real the dynamical matrix is positive definite, which implies the positive definiteness of the Hessian matrix and that a true minimum has been reached. All the eigenfrequencies, were found to be real so we are confident that the structure converged to a local minimum and not a saddle point. The structures were also examined visually to verify their reasonableness. Once the minimization converged, GULP was also used to calculate the phonon dispersion of the optimized crystal lattice. The full anisotropic phonon dispersions for all branches were calculated across the entire Brillouin zone. The dispersions were calculated by evaluating the square roots of the dynamical matrix eigenvalues across an evenly spaced grid of 1000 points that span the positive octant of the Brillouin zone.

### D. Thermal property calculations

The phonon dispersions were then used with semiempirical relaxation time expressions, to fit the thermal conductivity data. The starting point for this procedure was the following expression for thermal conductivity:

$$k_j = \sum_{\vec{K}p} c_p(\vec{K})[v_p(\vec{K}) \bullet \hat{j}]^2 \tau_p(\vec{K}). \quad (1)$$

The summation goes over all phonon wave vectors $K$ in the Brillouin zone and dispersion branches $p$, so it is a sum over all phonon states. $c_p(\vec{K})$ is the specific heat of all the phonons in a mode, $v_p(\vec{K})$ is the group velocity of a phonon in a given mode and it is projected onto the direction of interest, and $\tau_p(\vec{K})$ is the relaxation time, which is the time it takes an over excited phonon state to return to equilibrium. The modal phonon specific heat was calculated in the harmonic approximation with the following expression:

$$c_p(\vec{K}) = k_b\left(\frac{\hbar\omega_p(\vec{K})}{k_bT}\right)^2 \frac{\exp\left(\frac{\hbar\omega_p(\vec{K})}{k_bT}\right)}{\left(\exp\left(\frac{\hbar\omega_p(\vec{K})}{k_bT}\right)-1\right)^2}. \quad (2)$$

The group velocity is the gradient of the dispersion surface; hence phonon group velocities were estimated by taking the finite difference derivatives of the dispersion.

The phonon relaxation time is the time it takes a phonon mode that is out of equilibrium to return to equilibrium. The phonon relaxation time is different from the phonon lifetime, which is the average time a phonon exists before it is destroyed by a scattering event. For example, if a phonon mode were to have a high normal scattering rate and a low Umklapp scattering rate, it could have a small phonon lifetime and a large phonon relaxation time. In order to calculate the phonon relaxation time from first principles, the phonon lifetimes need to be calculated and the relationship between phonon lifetime and relaxation time needs to be known. Unfortunately, the relationship between phonon relaxation time and lifetime is not well understood. There are a number of models and approximations that are used to determine this relationship,[25–28] but little or no work has been done to rigorously test the validity and differences of the different models. The single mode relaxation time model, which simply approximates the phonon relaxation time as being equal to the phonon lifetime, has successfully been used to calculate the thermal conductivities of solid argon[29] and silicon.[30] However, its validity for different or more complex materials has never been tested; in addition, there are no known criteria that can be used to determine its validity. No other models that approximate the relationship between phonon relaxation time and lifetime have been rigorously tested with first principles calculations for any materials. Calculations of phonon lifetimes from first principles have been performed for simple materials like solid argon[29] and silicon.[30] However, even the calculations for such simple materials are very involved and many of the common assumptions that are used to perform these calculations may not be valid for complex materials like zeolites. For instance, the two most common assumptions used to calculate and estimate phonon lifetimes in a perfect crystal are: (1) phonon lifetimes can be adequately calculated by applying first-order time-dependent perturbation theory (i.e., Fermi's Golden Rule) to the anharmonic terms in the crystal Hamiltonian and (2) only the third-order anharmonic contribution to the crystal Hamiltonian induces significant phonon scattering. If this set of assumptions was true, then the phonon line broadening would be Lorentzian.[31] By performing molecular dynamics simulations and calculating normal mode autocorrelation functions, Chen and Kopelevich[32] have simulated phonon line broadening of some phonon modes in the zeolite sodalite; they found that some phonon line shapes deviate strongly from Lorentzian curves. While it is difficult to determine exactly which of the two assumptions have broken down, it is clear from the simulated phonon line broadening that at least one of them are invalid. Furthermore, even if the aforementioned assumptions were valid for calculating phonon lifetimes in zeolites from first principles, the large unit cells would result in the calculation being computationally intractable. There are molecular dynamics studies that explicitly calculate phonon lifetimes[32–34] without the aforementioned assumptions. However, this approach requires a large number of simulations with varying system sizes in order to adequately sample the Brillouin zone, so the calculation is computationally intractable for zeolites like LTA. In addition, the relationship between lifetime and relaxation time would have to be known in order to calculate the thermal conductivity.

A detailed first principles analysis of the phonon relaxation time in zeolites would require great leaps in the current understanding of phonon scattering and massive amounts of computer time. Therefore, the relaxation time was modeled using semiempirical formulas. Like other ordered and partially disordered zeolites[11,12,35,36] the thermal conductivity of LTA has a temperature dependence that is neither typical of a crystalline material nor of an amorphous material, but rather a mix of the two. It exhibits a temperature dependence that is close to what is observed for a "minimum thermal conductivity material," which is often modeled with phonons having the same fixed relaxation length regardless of mode or temperature. Attempts to fit the thermal conductivity of LTA with a "minimum thermal conductivity" model have revealed that a small temperature-dependent term needs to be included to adequately model the thermal conductivity. Thus, the relaxation time is modeled assuming phonon modes relax by both fixed relaxation length and temperature-dependent scattering mechanisms. The validity and shortcomings of this approach will be discussed in the results section.

The fixed relaxation length scattering term used is the same that would be used for boundary scattering and is[37]

$$\tau_B^{-1} = \frac{v}{l_{\text{eff}}}, \quad (3)$$

$l_{\text{eff}}$ is treated as a fitted constant. The temperature-dependent scattering term used is[38]

$$\tau_U^{-1} = B\omega^2 T e^{-\theta_D/3T}. \quad (4)$$

Here, $B$ is a fitted constant that is ascertained by fitting the thermal conductivity model to experimental data. $\theta_D$ is the Debye temperature, which is obtained by fitting the Debye model to experimental specific heat data. The exponent in the above expression has been treated as a fitted constant in pre-

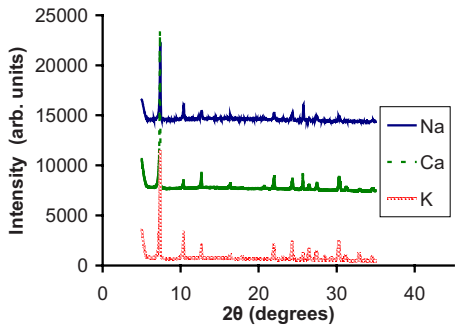


FIG. 2. (Color online) XRD patterns of LTA zeolite films containing different nonframework metal cations ($Na^+$, $Ca^{2+}$, and $K^+$).

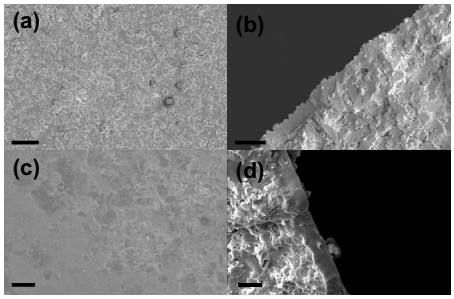


FIG. 3. SEM images of LTA zeolite films: (a) top view of film before polishing, (b) cross section view of film before polishing, (c) top view of polished film, and (d) cross section view of polished film. The scale bars equal 2 μm.

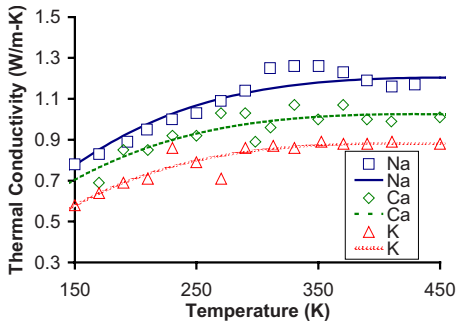


FIG. 4. (Color online) Measured (symbols) and model-fitted (curves) thermal conductivity of LTA zeolite films containing different nonframework metal cations ($Na^+$, $Ca^{2+}$, and $K^+$).

vious works.[39] However, the temperature-dependent scattering term is too small (when compared to the degree of precision of the measurements) to make the value of the exponent particularly significant. The above expression was developed for acoustic phonon scattering in simple materials, but it has two key features that make it suitable to quantitatively include in the present work. In the high temperature limit it will cause the thermal conductivity to be inversely proportional to temperature, which is the thermodynamically expected behavior for a crystalline material.[37] It also causes scattering to increase with phonon frequency, a trend that is intuitively expected. The expression for total relaxation time was calculated from Matthiessen's rule, which gave an overall scattering rate of

$$\tau^{-1} = \tau_U^{-1} + \tau_B^{-1}. \tag{5}$$

Matthiessen's rule is commonly used[28,37] and likely introduces little error into the calculation. Finally, to calculate the thermal conductivity the semiempirical expressions and Matthiessen's rule were inserted into Eq. (1) and fitted to experimental data. This procedure was carried out for the three different types of LTA studied here.

## III. RESULTS AND DISCUSSION

### A. Zeolite film structure and morphology

All the LTA films show a (200) out of plane orientation as determined by XRD (Fig. 2). Figure 3 shows the SEM cross section and top views of polished and unpolished LTA films. As expected, the morphology of the films is not altered upon ion exchange. The thickness of the LTA films is about 6 $\mu$m after six days of hydrothermal synthesis. These films are thicker than previously reported LTA films.[18] This is likely due to the higher synthesis temperature used in this study. The final thicknesses of the polished LTA films are between three and five microns. The composition of the films was investigated by EDS measurements taken from a number of points in the film cross section (Table I). All the films show a Si/Al ratio of approximately 1 within experimental error. As desired, the Al/cation ratio is about unity for the univalent cations $Na^+$ and $K^+$, and about 2 for the divalent cation $Ca^{2+}$.

TABLE I. LTA film compositions for three different nonframework cations.

| Sample name | Si/Al | Al/cation | Si/cation |
|---|---|---|---|
| Na-LTA | $1.18 \pm 0.17$ | $1.3 \pm 0.21$ | $1.52 \pm 0.13$ |
| K-LTA | $1.33 \pm 0.15$ | $1.27 \pm 0.2$ | $1.69 \pm 0.28$ |
| Ca-LTA | $1.42 \pm 0.2$ | $1.87 \pm 0.7$ | $2.6 \pm 0.7$ |

### B. Fit of the thermal conductivity

The fitted thermal conductivity is shown in Fig. 4. The magnitudes and temperature dependence of the thermal conductivities for all three types of LTA are typical for nanoporous crystals.[36,40] At moderate temperatures the thermal conductivities continue to increase, and the temperature dependences of the thermal conductivities are similar to that of the specific heats as shown in Fig. 5. This implies that phonon mean free paths in LTA have weak temperature dependences. The continued rise of the thermal conductivity at the temperatures shown implies that the optical modes contribute substantially to the thermal conductivity. This is because all the acoustic phonons in LTA have reached the classical limit even at 150 K, so their contribution to the thermal conductivity likely decreases with increasing temperature. The physical parameters obtained from fitting the model to the data, and their 95% confidence intervals expressed as a percentage of their values, are shown in Table II. It is clear that the boundarylike scattering is the dominant phonon scattering mechanism, which explains the weak temperature dependencies of the phonon relaxation lengths. The fitted values of $l_{\text{eff}}$ have small confidence intervals. This suggests that the assumed functional form of the temperature-independent scattering term is physically relevant. The moderately large

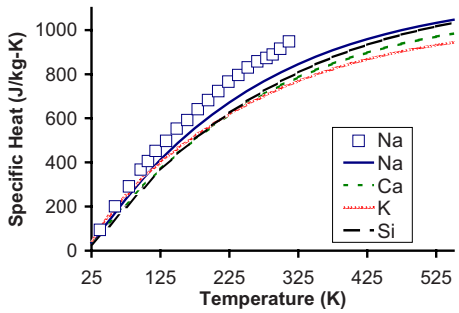


FIG. 5. (Color online) Calculated specific heat (curves) of zeolite LTA structures including Na-LTA, Ca-LTA, K-LTA, and pure-silica LTA; and comparison with experimental data (symbols) for Na-LTA from the literature.

TABLE II. Physical parameters obtained from fitting the thermal conductivity model to our experimental data. Each 95% confidence interval (error bar) is expressed as a percentage of the corresponding physical parameter value.

| Cation | Fitted constant | Fitted value | Confidence intervals (%) |
|---|---|---|---|
| Na | $B$(s/rad$^2$ K) | $2.66\times10^{-21}$ | 64 |
| Na | $l_{\text{eff}}$(nm) | 11.6 | 8 |
| K | $B$(s/rad$^2$ K) | $6.78\times10^{-21}$ | 64 |
| K | $l_{\text{eff}}$(nm) | 7.45 | 8 |
| Ca | $B$(s/rad$^2$ K) | $2.63\times10^{-21}$ | 67 |
| Ca | $l_{\text{eff}}$(nm) | 10.07 | 7 |

confidence intervals for the fitted constants used in the temperature-dependent scattering terms indicate that there are inaccuracies in the assumed functional form of the temperature-dependent scattering. The temperature-dependent scattering is not as significant as the temperature-independent boundarylike scattering. For example, we have made thermal conductivity fits that include only the boundarylike scattering term. It was found that the inclusion of a temperature-dependent scattering term is necessary to reproduce the correct temperature dependence, but neglecting the temperature-dependent scattering term does not greatly change the values of the fitted boundarylike scattering constants. The fitted constants for boundarylike scattering are about 15% less than the values obtained in the original fits. As a result, it is concluded that changing the exponent will only have a small effect on the values of the fitted constants. Thus, even if a more accurate temperature-dependent scattering term were available, its fitted parameters would likely have large confidence intervals as well.

The present results on zeolite LTA are qualitatively similar to those obtained in zeolite MFI[36,41] and may be indicative of a more general thermal transport behavior in zeolites. The weak temperature dependence of the phonon scattering is also evident in molecular simulations preformed by McGaughey and Kaviany[11] on perfectly ordered siliceous LTA. It is an inherent characteristic of its structure, and not a product of the disorder in the cation locations. The weak temperature dependence implies that phonon relaxation times in LTA are only weakly dependent on phonon occupation numbers, and is consistent with a boundarylike scattering mechanism dominating the thermal conductivity. Furthermore, McGaughey and Kaviany[11] have observed trapping of heat between the zeolite pores in their simulations. This shows that the pores play a critical role in limiting heat conduction in zeolites. This finding is not surprising. Heat conduction can be envisioned as a random walk of energy along a lattice network, and therefore pores in the lattice will greatly limit the transport of heat. In addition, the fitted values of $l_{\text{eff}}$ are not much greater in magnitude than the length scales of the pore network. As a result, it can be deduced that the pores play a major role in phonon scattering.

### C. Specific heat of zeolite LTA

The calculated specific heat is shown in Fig. 5. The experimental specific heat of Na-LTA, which has previously been measured by Qiu *et al.*,[42] is also shown. There are small but significant deviations between Qiu's data and our calculations. Using the same interatomic potential and techniques similar to those presented here, the specific heats of pure-silica quartz, zeolite MTT, and zeolite MFI have been calculated with high accuracy.[43] The aforementioned materials are all composed of pure-silica frameworks. LTA is composed of an aluminosilicate framework and nonframework cations, so the deviations between the calculated and experimentally measured specific heat of Na-LTA may result from an inadequate description of the Al–O interactions or the Na–O interactions. It may also be indicative of the loosely bound cations undergoing large, anharmonic oscillations that are not captured in the harmonic lattice dynamical calculations. While it is likely that cation thermal motion is largely anharmonic, it would take a tremendous amount of anharmonicity to account for the deviations between the model and experiment because only about 15% of the atoms in Na-LTA are extra-framework cations. The deviations between the calculated and measured specific heat of Na-LTA are larger than the deviations in the calculated specific heats between the different types of LTA. Therefore it is unclear if the calculated differences in specific heat between the different types of LTA indicate that the specific heats are actually different from each other or if the differences result from inaccuracies in the harmonic model of specific heat or the interatomic potential.

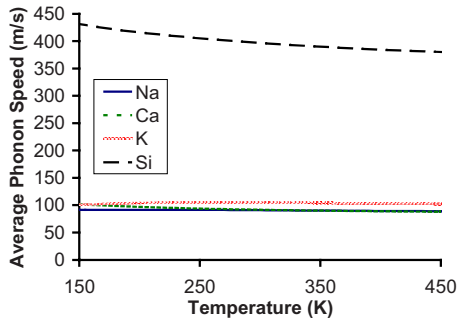


FIG. 6. (Color online) Calculated specific-heat-weighted mean phonon speeds of zeolite LTA structures including Na-LTA, Ca-LTA, K-LTA, and pure-silica LTA.

### D. Phonon speed and mean free path

The specific-heat-weighted phonon speed is shown in Fig. 6. Analyzing this quantity can give some insight into the thermal behavior and phonon dynamics of zeolite LTA. The average phonon velocities are nearly temperature-independent and very low in comparison to a pure-silica zeolite such as MFI.[9] The low temperature dependence and small magnitudes of the average phonon speeds imply that different optical branches have similar phonon speeds and that the optical branches are relatively flat throughout the Brillouin zone. The differences in phonon speed between the different types of aluminosilicate LTA are quite small. This implies that the differences in thermal conductivity between the different types of LTA primarily result from different boundary scattering rates, which result in different phonon mean free paths. However, it is not apparent why different

types of LTA have different phonon boundary scattering rates. The three types of LTA are too different from each other to be thought of as perturbations of one another, and so a direct comparison of the same phonon mode in the different types of LTA is not possible. The room temperature thermal conductivities of Na-LTA, K-LTA, and Ca-LTA are 1.14, 0.85, and 0.98 W/m/K, respectively. Neither silica framework density, mass density, degree of cation disorder, cation mass, nor even cation valency correlate with the trend of thermal conductivity across the different types of LTA.

The effects of inclusion of nonframework molecules in zeolite pores on phonon dynamics have been studied by Chen and Kopelevich.[32] It was found that the inclusion of molecules inside sodalite pores does not qualitatively change the phonon dynamics. However, the mean values of the normal mode coordinates, phonon lifetimes, and phonon frequencies can change. The study also showed that nonframework molecules and atoms located in the pores can lengthen the lifetimes of some phonon modes and shorten the lifetimes of other phonon modes, so nonframework molecules have a complicated relationship with phonon dynamics and do not act as mere point scatters that reduce phonon lifetimes. Murashov[12] used molecular simulations to analyze the effects of nonframework cation mass on thermal conductivity and found a complex periodic relationship between cation mass and thermal conductivity. The aforementioned studies have shown that the relationship between nonframework cation and thermal conductivity is highly complex. Therefore it is not surprising that the model used here, which treats phonon scattering in an approximate manner due to computational necessity, cannot fully interpret how and why different nonframework cations affect the thermal conductivity of LTA.

The phonon mean free paths are likely of the same order of magnitude as the phonon relaxation lengths, which are of the order of a few lattice constants. Although previous researchers[34,44] state that phonons with mean free paths shorter than their wavelengths are not physically meaningful, one can always sum over enough normal modes of vibration to create a well-defined packet of energy in space; albeit for small mean free paths the wave vector of a phonon may have a large amount of uncertainty. With regard to the phonon lifetime, Klemens[45] states that phonons with lifetimes shorter than their periods are also not physically meaningful, although no rigorous justification was provided for this argument. However, there is certainly a question as to how much spatial and temporal uncertainty a phonon can have and still adequately describe thermal transport. Peierls[46] has derived the following criterion for the minimum mean free path a phonon can have and still be used to describe thermal transport:

$$l_{mfp} > \frac{\hbar v}{k_B T}. \tag{6}$$

This criterion was derived by reasoning that the uncertainty in phonon energy should be small enough, so that it does not add significant uncertainty to its occupation number. The phonons in LTA satisfy this criterion. However, the work of Peierls only considered the effect of uncertainty of phonon occupation numbers, but not other quantities that influence phonon scattering rates such as the Fourier-transformed anharmonic spring constants. Almost all the phonons in LTA have relaxation times significantly longer than their periods; therefore any frequency-dependent quantities that appear in phonon scattering rates will not introduce significant error. However, phonons in LTA do possess small mean free paths, and hence there is a moderate amount of uncertainty in their wave vectors. The uncertainty in wave vector can cause phonon collisions that do not satisfy the conservation of quasimomentum. The uncertainty in phonon wave vector can also propagate and cause uncertainty in the Fourier-transformed anharmonic spring constants. Neither phenomenon is well understood, and both furnish important theoretical questions. The model presented here assumes that scattering rates are only frequency-dependent and do not depend explicitly on wave vector. Furthermore, the model treats all scattering process as contributing directly to the thermal resistivity, and does not differentiate between normal and Umklapp scattering processes. As a result the uncertainty in phonon wave vector is not expected to have a significant effect on the model results.

### E. Validity of the Boltzmann transport equation for LTA

The unusual temperature dependence of the thermal conductivity of LTA, and its large unit cell, lead to the question whether the Boltzmann transport equation is a suitable way to model its thermal conductivity. Allen and Feldman[47] have developed a thermal conductivity model for use with disordered materials, which could potentially yield the observed temperature dependence. However, their model is only applicable for materials that have a quantum density matrix that has large nondiagonal elements. For a perfectly ordered material the quantum density matrix is diagonal, and simulations of perfectly ordered siliceous LTA also yield scattering rates with weak temperature dependences. Therefore, the off-diagonal elements in the heat flux operator do not cause the weak temperature dependence. As a result, the Allen–Feldman model is inapplicable. Phonon hopping models have also been developed,[48] but they are intended for use with amorphous and strongly disordered materials. There is no well-defined reason to believe that the Boltzmann transport equation is not valid for zeolites. As mentioned earlier, the phonon relaxation lengths are only on the order of a few lattice constants, but this is not problematic if one is willing to accept some uncertainty in the phonon wave vectors. Furthermore, phonon slowing has previously been shown to be a crucial factor in the reduction of thermal conductivity of zeolite MFI by the addition of impurities,[36] and this is further evidence that the Boltzmann transport equation is valid.

## IV. CONCLUSIONS

We have systematically studied the effect of temperature and extra-framework cations on the thermal properties of zeolite LTA. We successfully synthesized continuous zeolite LTA films and ion exchanged them with various metal cations, to obtain samples suitable for high-quality thermal con-

ductivity measurements. The thermal conductivities of these films were successfully measured for the first time, using the three-omega method. A modeling approach, previously developed for zeolite MFI, which uses semiempirical relaxation time scattering rates along with full anisotropic dispersion, has been modified and implemented to calculate the thermal properties of LTA and to analyze its phonon dynamics. The results validated important aspects of the modeling approach and also suggested its limitations. Optical phonons dominated the thermal conductivity and boundarylike scattering associated with the pore network was found to be the strongest phonon scattering mechanism, as also observed in MFI zeolite. Our approach was previously able to explain how small amounts of framework aluminum influence the thermal conductivity of zeolite MFI. However, it was unable to fully explain how each type of metal cation influences the thermal conductivity of zeolite LTA. Despite the shortcomings of the present model, this approach still provided insight into heat transport in nanoporous materials and has been shown to be transferable to multiple materials.

## ACKNOWLEDGMENTS

We acknowledge partial support for this work from NSF (Grant No. CBET-0436721), and A. G. Ahmadi (Georgia Tech) for assistance with heater microfabrication.

[1]C. Baerlocher, L. B. McCusker, D. Olson, and W. M. Meier, International Zeolite Association, *Atlas of Zeolite Framework Types*, 6th rev. ed. (Elsevier, Amsterdam, 2007).
[2]M. E. Davis, Nature (London) **417**, 813 (2002).
[3]M. Tsapatsis, AIChE J. **48**, 654 (2002).
[4]Z. J. Li, M. C. Johnson, M. W. Sun, E. T. Ryan, D. J. Earl, W. Maichen, J. I. Martin, S. Li, C. M. Lew, J. Wang, M. W. Deem, M. E. Davis, and Y. S. Yan, Angew. Chem., Int. Ed. **45**, 6329 (2006).
[5]M. Sun, W. Maichen, R. Pophale, Y. Liu, R. Cai, C. M. Lew, H. Hunt, M. W. Deem, M. E. Davis, and Y. Yan, Microporous Mesoporous Mater. **123**, 10 (2009).
[6]C. M. Lew, Z. J. Li, S. Li, S. J. Hwang, Y. Liu, D. I. Medina, M. W. Sun, J. L. Wang, M. E. Davis, and Y. S. Yan, Adv. Funct. Mater. **18**, 3454 (2008).
[7]Z. Yang, Y. Xia, and R. Mokaya, Chem. Mater. **17**, 4502 (2005).
[8]K. Mukhopadhyay, A. Koshio, N. Tanaka, and H. Shinohara, Jpn. J. Appl. Phys., Part 2 **37**, L1257 (1998).
[9]V. V. Murashov and M. A. White, Mater. Chem. Phys. **75**, 178 (2002).
[10]A. Griesinger, K. Spindler, and E. Hahne, Int. J. Heat Mass Transfer **42**, 4363 (1999).
[11]A. J. H. McGaughey and M. Kaviany, Int. J. Heat Mass Transfer **47**, 1799 (2004).
[12]V. V. Murashov, J. Phys.: Condens. Matter **11**, 1261 (1999).
[13]P. K. Schelling, S. R. Phillpot, and P. Keblinski, Phys. Rev. B **65**, 144306 (2002).
[14]X. W. Zhou, S. Aubry, R. E. Jones, A. Greenstein, and P. K. Schelling, Phys. Rev. B **79**, 115201 (2009).
[15]K. V. Tretiakov and S. Scandolo, J. Chem. Phys. **120**, 3765 (2004).
[16]V. Subramanian and K. Seff, J. Phys. Chem. **81**, 2249 (1977).
[17]R. Y. Yanagida, A. A. Amaro, and K. Seff, J. Phys. Chem. **77**, 805 (1973).
[18]L. C. Boudreau, J. A. Kuck, and M. Tsapatsis, J. Membr. Sci. **152**, 41 (1999).
[19]G. V. Lewis and C. R. A. Catlow, J. Phys. C **18**, 1149 (1985).
[20]J. J. Pluth and J. V. Smith, J. Am. Ceram. Soc. **105**, 1192 (1983).
[21]J. J. Pluth and J. V. Smith, J. Am. Ceram. Soc. **102**, 4704 (1980).
[22]J. J. Pluth and J. V. Smith, J. Am. Ceram. Soc. **83**, 741 (1979).
[23]C. R. A. Catlow, C. M. Freeman, M. S. Islam, R. A. Jackson, M. Leslie, and S. M. Tomlinson, Philos. Mag. A **58**, 123 (1988).
[24]J. D. Gale, J. Chem. Soc., Faraday Trans. **93**, 629 (1997).
[25]J. Callaway, Phys. Rev. **122**, 787 (1961).
[26]P. G. Klemens, Solid State Phys. **7**, 1 (1958).
[27]G. P. Srivastava, Pramana **6**, 1 (1976).
[28]G. P. Srivastava, *The Physics of Phonons* (Adam Hilger, Bristol, UK, 1990).
[29]J. E. Turney, E. S. Landry, A. J. H. McGaughey, and C. H. Amon, Phys. Rev. B **79**, 064301 (2009).
[30]J. E. Turney, A. J. H. McGaughey, and C. H. Amon, Phys. Rev. B **79**, 224305 (2009).
[31]D. C. Wallace, *Thermodynamics of Crystals* (Dover, New York, 1972).
[32]C. Y. Chen and D. I. Kopelevich, Mol. Simul. **34**, 155 (2008).
[33]A. J. C. Ladd, B. Moran, and W. G. Hoover, Phys. Rev. B **34**, 5058 (1986).
[34]A. J. H. McGaughey and M. Kaviany, Phys. Rev. B **69**, 094303 (2004).
[35]A. M. Greenstein, S. Graham, Y. C. Hudiono, and S. Nair, Nanoscale Microscale Thermophys. Eng. **10**, 321 (2006).
[36]Y. Hudiono, A. Greenstein, C. Kuete, B. Olson, S. Graham, and S. Nair, J. Appl. Phys. **102**, 053523 (2007).
[37]J. M. Ziman, *Electrons and Phonons* (Claredon, Oxford, 1960).
[38]G. A. Slack and S. Galginaitis, Phys. Rev. **133**, A253 (1964).
[39]M. Asen-Palmer K. Bartkowski, E. Gmelin, M. Cardona, A. P. Zhernov, A. V. Inyushkin, A. Taldenkov, V. I. Ozhogin, K. M. Itoh, and E. E. Haller, Phys. Rev. B **56**, 9431 (1997).
[40]B. L. Huang, Z. Ni, A. Millward, A. J. H. McGaughey, C. Uher, M. Kaviany, and O. Yaghi, Int. J. Heat Mass Transfer **50**, 405 (2007).
[41]A. M. Greenstein, Y. C. Hudiono, S. Graham, and S. Nair, Proceedings of the ASME International Mechanical Engineering Congress and Exposition, Seattle, WA, 2007, pp. 625–630.
[42]L. Y. Qiu, V. Murashov, and M. A. White, Solid State Sci. **2**, 841 (2000).
[43]A. Greenstein, Y. Hudiono, S. Nair, and S. Graham, Proceedings of the ASME International Mechanical Engineering Congress and Exposition, Chicago, IL, 2006, pp. 415−421.
[44]J. R. Olson, R. O. Pohl, J. W. Vandersande, A. Zoltan, T. R. Anthony, and W. F. Banholzer, Phys. Rev. B **47**, 14850 (1993).
[45]P. G. Klemens, Phys. Rev. **122**, 443 (1961).
[46]R. E. Peierls, *Quantum Theory of Solids* (Oxford University Press, New York, 1954).
[47]P. B. Allen and J. L. Feldman, Phys. Rev. B **48**, 12581 (1993).
[48]T. Damker, H. Bottger, and V. V. Bryksin, Phys. Rev. B **59**, 8626 (1999).